UNIVERSITY OF TWENTE.

Faculty of Engineering Technology,
Water Engineering & Management,
Marine & Fluvial Systems

Erosion and transport processes of mixed sediments

Literature report

Van Thi To Nguyen

February 2025

CE&M research report 2025R-002/WEM-002
ISSN 1568-4652

Literature report:

Erosion and transport processes of mixed sediments

Van Thi To Nguyen

February 2025

Supervisors:

Dr. Ir. P.C. Roos
Dr. Ir. J.J. van der Werf

Marine and Fluvial Systems Group
Department of Civil Engineering
University of Twente

CE&M research report 2025R-002/WEM-002
ISSN 1568-4652

Acknowledgements

This study is a part of the SEDIMARE (*Sediment transport and morphodynamics in marine and coastal waters with engineering solutions*) project and is funded by a Horizon Europe Marie Skłodowska-Curie Actions Doctoral Networks. The author thanks the supervisors, Jebbe van der Werf and Pieter Roos, for their thorough feedback and guidance.

Contents

1. INTRODUCTION

1.1 BACKGROUND

Sediment transport is a consistently significant research area, particularly for countries with low-lying topography with large river deltas or long coastlines such as the Netherlands and Vietnam. People have and will always try to understand how sediment transports, erodes, and settles in order to predict morphological changes. Therefore, following that research path, the SEDIMARE project was established by the European Union to create a comprehensive research group on sediment transport, morphodynamics and sustainable coastal engineering solutions. As part of the SEDIMARE project, the SEDIMARE #3 study aims to gain understanding about erosion and transport of sand – silt mixtures. This literature is a starting point of that study.

Over the past few decades, there have been many empirical models used to describe and predict erosion and transport of sediment. Traditionally, these models mainly treat sand (grain diameters D between 63 and 2000 μm) and finer particles such as silt and clay, collectively referred to as mud or fines ($D < 63$ μm) separately (e.g. Partheniades, 1965; Van Rijn, 1993). The reason for this separation is that sands and muds have different behaviors, particularly, sand behaves as non-cohesive sediment while mud has cohesive properties (i.e. particles tend to stick together as aggregates). However, natural sediments (especially in coastal areas) are usually a combination of sand and mud. Thereby, complexities arise due to the interactions between the cohesive (mud) and non-cohesive (sand) fractions.

To achieve the goal of the SEDIMARE #3 project as well as to enhance our understanding sediment processes and characteristics of mixed sediment, especially sand-silt mixtures, we will apply datasets from laboratory experiments. This literature review forms the start of the research.

1.2 OBJECTIVES AND LITERATURE QUESTIONS

This literature review will address the following questions:

Q1: What are the (physical) characteristics of coastal systems in which the beds are composed of both sand and mud?

Q2: Which physical processes control the erosion and transport of sand-mud?

Q2.1: What is the difference between the erosion and transport of sand-mud mixtures compared to the pure sand/mud transport?

Q2.2: What is the relative importance of waves and currents for the erosion and transport of sand-mud mixtures?

Q3: Which laboratory experiments have been carried out to study the erosion and transport of sand-mud mixtures?

Q4: Which empirical formulas exist to compute the erosion and transport of sand-mud mixtures?

1.3 OUTLINE

This literature review is organized as follows. The topic is introduced and the literature search questions are posed in Chapter 1. Chapter 2 discusses coastal systems which contain the sand – mud mixtures and their characteristics (Q1). To answer the second question, Chapter 3 first introduces the main sediment and soil properties before discussing the relevant physical processes of mixed sediments in Chapter 4. This includes the interaction of waves and currents with the sediment, governing the erosion of mixed sediment from the bed, and the subsequent transport (Q2). Chapter 5 gives a review of existing laboratory experiments on sand – mud mixtures (Q3). Furthermore, Chapter 6 presents existing practical sand-mud mixtures models (Q4). Finally, Chapter 7 presents the conclusion of this literature review by answering the literature search questions, and by doing so, reveals the knowledge gap on understanding and practical modeling of sand-mud in coastal environments.

2. MIXED-SEDIMENT COASTAL SYSTEMS

Sand-mud mixtures which we are considering are mixed sediments consisting of fine particles below 2 mm such as sand, silt and clay. These sediments are typically found in coastal systems or downstream areas where sediment is weathered and eroded from coarser to finer size In particular, sand-mud or sand-silt mixtures can be found widely in estuaries and tidal basins. Depending on the mass percentages of clay and slit in the bed one can distinguish between clay-dominated (clay-silt ratio ≥ 2) and silt-dominated systems (clay-silt ratio ≤ 0.5) following the traditional classification of Folk (1954). Furthermore, there is no accurate way to identify/distinguish between these two systems. Notable silt-rich systems are the Yellow River, Yangtze River (both China), and the Mekong Delta (Vietnam) (Figure 1). Examples of clay-dominated coastal systems are the Wadden Sea (The Netherlands), Mississippi Delta (USA), and Amazon Delta (Brazil). These systems offer valuable ecosystems and agricultural land due to the fertile fine particles (silt and clay) and organic materials (e.g., active bacteria, fungi, and organic molecules), providing essential nutrients for plant growth.

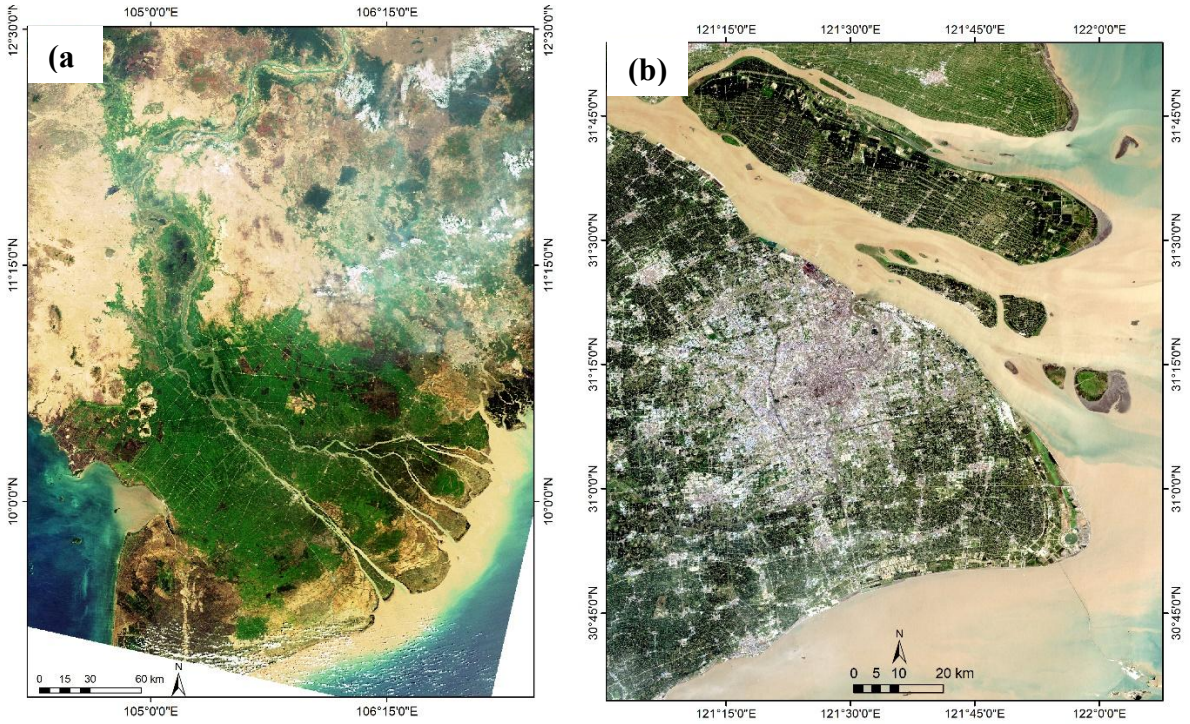

Figure 1. Satellite images of the Mekong Delta (a) taken by Envisat and the Yangtze delta (b) taken by Shanghai Landsat 7, respectively.

2.1 SILT-DOMINATED SYSTEMS

In this section, some notable silt-rich systems are introduced such as Yangtze and Yellow River deltas (China) and Mekong delta (Vietnam). A similar point between these

deltas is that a large river system is the main sediment source. Eroded by the river branches extending across the continent, the amount of sediment these deltas discharge into the ocean each year can reach up to millions of tons per year (Unverricht et al., 2013; Anthony et al., 2015; te Slaa, 2020; Tian et al., 2021). Most of the silt in the Yellow River comes from the central China Loess Plateau. The sediment in the Yellow River and Yangtze River has similar clay mineral distributions, reflecting their common source in the Tibetan Plateau (te Slaa, 2020). The Yangtze estuary is divided into the North Branch and South Branch by Chongming island. By taking samples around Chongming island, te Slaa (2020) found that the south-eastern tidal flat contains more non-cohesive sand-silt mixtures compared to the silt-dominated north-eastern side of Chongming island. The clay content in the south-eastern area is below 10% whereas it can reach up to 20% in the north-eastern tidal flat. On the other hand, sediment in the Yellow River was found to be non-cohesive, ranging from sand-dominated to silt-dominated regime with a maximum clay content below 6% (te Slaa, 2020).

Another silt-rich system is the Mekong River Delta (Vietnam). This is a tide-dominated delta following the triangular classification of deltaic depositional systems (Nguyen et al., 2000). Sediment distribution in the Mekong Delta used to be controlled by monsoon-driven river discharge, waves, along-shore currents, and tides. However, nowadays, there is a significant decrease in sediment supply to the coast of the Mekong Delta due to dam retention of sediment in the upstream region, as well as shoreline erosion likely linked to large-scale commercial sand mining and groundwater extraction along river and delta channels (Anthony et al., 2015). By taking samples along five shore normal transects in the coastal zone of the Mekong Delta, Unverricht et al. (2013) found coarser grains in northern area (near Bassac river mouth) and sediments are found to be finer downward to the south area (from Bac Lieu to the Cape Ca Mau). This is mainly due to strong wind-induced along-shore currents during the winter monsoon season (from the northeast) which can wash suspended fine sediment from north to southwest areas. Furthermore, this winter monsoon wind-driven waves and along-shore currents can be weaker in the most southwest area (Cape Ca Mau). This, combined with sediment supply from eastern side of Mekong Delta (the side of Gulf of Thailand) , makes Cape Ca Mau a depositional place with percentages of silt and clay larger than 90% (Tamura et al., 2010; Unverricht et al., 2013).

2.2 CLAY-DOMINATED SYSTEMS

Differences between clay-dominated and silt-dominated systems not only depend on hydrodynamics (such as wind, waves, tidal currents) but also on the source of sediment. One notable clay-dominated coastal system is the

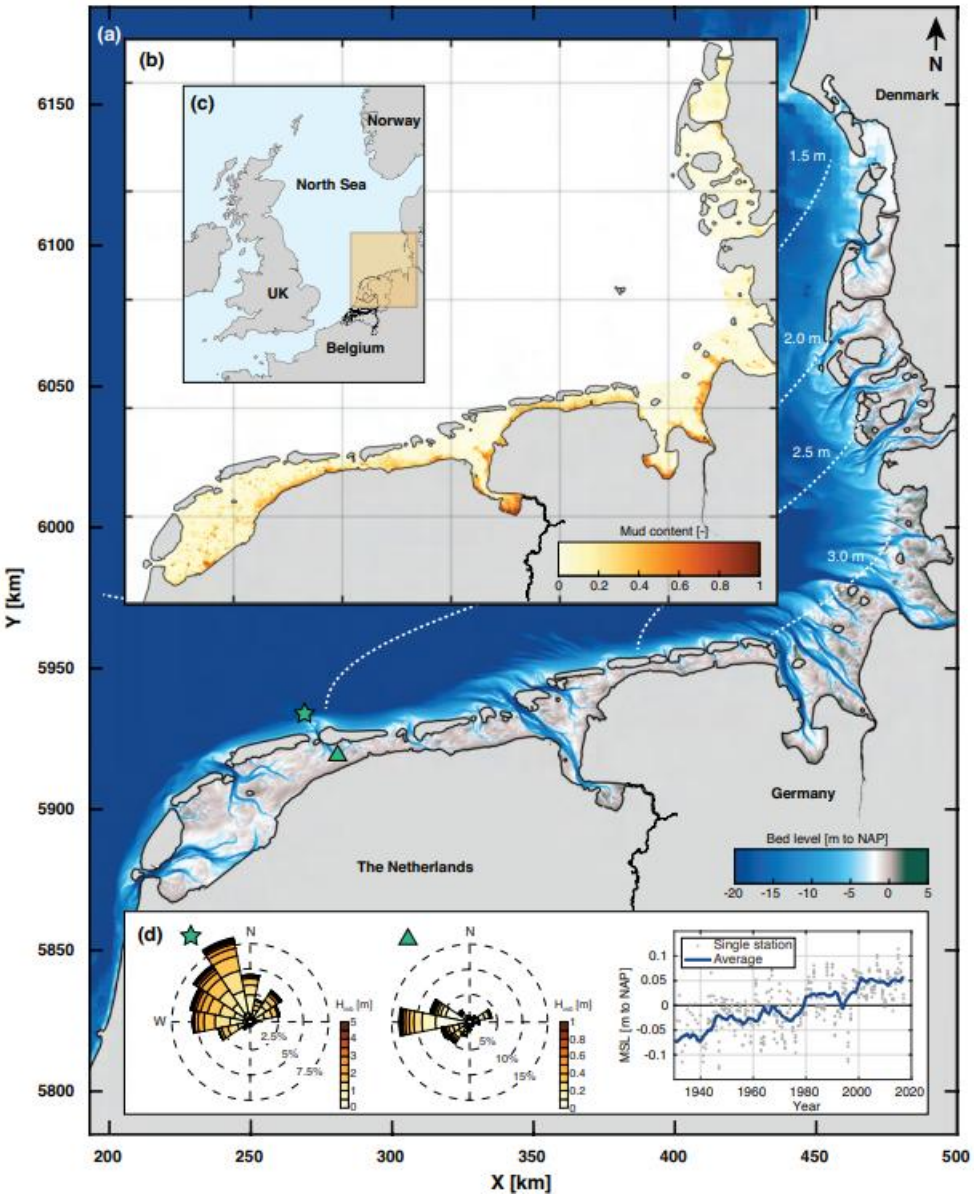

Figure 2. Overview map of the Wadden Sea. (a) Bathymetry map combined within 2015-2021. The white dotted lines indicate the tidal range. (b) Bed sediment composition plotted as the mud content in the upper bed (top 4–10 cm). The Danish part of the Wadden Sea is not included in the plot because there were no available data on this area. (c) Location of the Wadden Sea. (d) Example of a wave climate on an ebb-tidal delta and in a Wadden Sea basin (both calculated over the period 2015–2018), and average yearly mean sea level (MSL) from tide gauge records in the Dutch basins over the past century (figure taken from Colina Alonso et al., 2024)

Wadden Sea (Netherlands). The mud in the Wadden Sea mostly comes from the North Sea (original from the Dover Strait, in between France and the United Kingdom) by the North Sea Continental Flow (NSCF) (reference needed here). Beside marine mud sources, fluvial mud sources of the Wadden Sea are Lake IJssel (via the sluices den Oever and Kornwerderzand) and the Ems, Weser and Elbe estuaries (Colina Alonso et al., 2024). Tidal basins in the Wadden Sea are separated from the North Sea by barrier

islands which help to reduce wave strength, which facilitates the deposition or accumulation of fine sediments. According to Van Ledden (2003), the average mud content of the Wadden Sea is relatively low (less than 10%). Sand is found more near the mouth where tidal currents are stronger, whereas silt and clay deposit near borders where flow velocity approaches zero. With offshore waves generated in the North Sea (South East direction) and local wind-waves (mainly East direction) at outside and inside barriers (see Figure 2d surface mud sediments are mostly transported from the South West forwards to Northern part of Wadden Sea (Colina Alonso et al., 2024). Besides, Figure 2b shows the bed composition in the Wadden Sea. high mud contents are found deep inside rivers and along borders (e.g., Ems-Dollard, Weser).

3. BASIC DEFINITIONS OF SEDIMENT AND SOIL PROPERTIES

3.1 PARTICLE SIZE

Based on particle sizes, the sediment can be separated and defined into multiple types: gravel, sand, silt, and clay, corresponding to decreasing size, respectively. As this study focuses on sand and mud fractions, Table 1 only shows the particle size of sand and below. The particle size in Table 1 is showed under two scales including micrometer (μm) and Phi (ϕ) scale which is a logarithmic transformation of the grain diameter in millimeters ($\phi = -\log_2 D$) and commonly used in log scale graph. Coastal sediments without gravels primarily consist of two fractions: sand ($63 \leq D < 2000$ μm) and mud, encompassing silt and clay particles ($D < 63$ μm).

Particle size is the most important factor, along with particle shape, mineral composition, and moisture content, to define the cohesive properties of sediment. In particular, when considering saturated soil, where the pore water pressure is not primarily affected by capillary action or tension in the soil, larger particle sizes lead to larger void sizes of soil, promoting rapid drainage (drained conditions). Consequently, the pore pressure remains low; in the case of coarser soils like sand, this means that particle adherence is primarily due to friction and mechanical interlocking rather than cohesion. Conversely, smaller particles, as found in silt and clay, have smaller voids, impeding efficient drainage (undrained conditions), leading to higher pore pressure and increased particle cohesion. In undrained conditions, the pore water is difficult to escape or flow into the soil while the soil keeps being deformed, inducing local excess pore water (or negative) pore water pressure in the soil (depending on the sediment packing in the bed). As a result, particles will experience temporary suction from this local pore water pressure. This phenomenon is called as pseudo cohesion and is commonly encountered with silt (Winterwerp et al., 2021). Further discussions on cohesion/ cohesionless will be presented in section 3.2.

3.2 COHESION

Cohesion is a property of sediment, usually applied for fine-grained particles (such as clay and very fine silt). Cohesion is basically caused by three main factors: Van der Waals force (or molecular force), hydrogen bonds, and organic polymers. Firstly, the Van der Waals force is a weak molecular attractive force between particles that is proportional to grain size and inversely proportional to distance. Besides, clay minerals (kaolinite, illite and montmorillonite) are hydrous alumino-silicates which form flat hexagonal sheets. This shape differs from the more or less spherical shape of silt and sand which are primarily composed of silica (SiO_2). Therefore, for clay particles, which have a flaky shape that brings particles closer together compared to silt, the Van der Waals force becomes more significant. Additionally, the Van der Waals force is more

Table 1. Grain-size classification according to Wentworth (1922) for sand and mud only.

Wentworth Grade	**Size (μm)**	**Phi (ϕ) Scale**	**Sediment**	
Very coarse sand	1000 – 2000	0 to -1		
Coarse sand	500 – 1000	1 to 0		
Medium sand	250 – 500	2 to 1	**SAND**	
Fine sand	125 – 250	3 to 2		
Very fine sand	63 – 125	4 to 3		
Coarse silt	31 – 63	5 to 4		
Medium silt	16 – 31	6 to 5	**Silt**	
Fine silt	8 – 16	7 to 6		**MUD**
Very fine silt	4 – 8	8 to 7		
Clay	< 4	> 8	**Clay**	

dominant for fine particles (silt and clay) compared to gravitational forces because it decreases less with decreasing grain size (power of 2 versus power of 3 for gravity). Secondly, hydrogen bonding is induced by the negative charges (or electrostatic forces) on the surface of clay plate which can be compensated with cations in the ambient solution (Winterwerp and Van Kesteren, 2004). Thirdly, in clay-dominated environments, there are more organic materials compared to silty environments, where the main composition is still silica. This makes the cohesion of clay stronger due to the presence of organic polymers compared to silts. Therefore, in studies of sand-silt mixtures (or silty/ silt-dominated mixtures) that do not include very fine silt and clay, cohesion due to hydrogen bonding and organic polymers can be neglected, and the Van der Waals force is relatively more important (Winterwerp et al., 2022; Yao et al., 2022). Furthermore, cohesion is still observed for clay-size particles in experimental study of Roberts et al. (1998) even they only applied pure-quartz materials (commonly considered as non-cohesive materials).

In mixed-sediment beds, the most important parameters to define cohesive properties are particle size distribution, plasticity, bulk density and organic content following Parchure and Teeter (2003) and Parchure and Davis (2005). Firstly, the particle size distribution (PSD) is the most important parameter to determine non-cohesive and cohesive property of a sediment sample. The median grain size (D_{50}), as

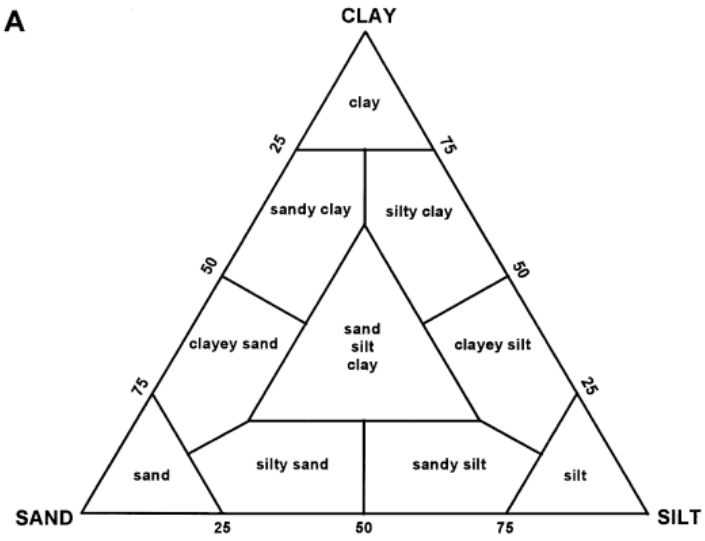

Figure 3. Traditional sediment triangle for sediment classification by Shepard (1954)

50th percentile of the PSD, is commonly used in computations of erosion, transport, settling and other sediment-related processes. Besides, the gradation parameter (or the standard deviation of PSD, σ_d) represents the sorting of a sediment mixture and can be calculated as $\sigma_d = D_{50}/D_{16} + D_{84}/D_{50}$ with D_{16}, D_{50} and D_{84} indicate for 16%, 50% and 84% of sediment fraction by weight in PSD. $\sigma_d < 1.35$ indicates a narrow PSD and a well-sorted sediment mixture and oppositely, $\sigma_d > 1.35$ shows a wide and poorly-sorted mixture. These parameters can work well for unimodal mixtures (PSD only has one peak), however, gradation cannot distinguish if there is two peaks in PSD (bimodal mixtures).

In another perspective, PSD in mixtures can be visualized by a three-component classification scheme, which is the so-called traditional sediment triangle (ternary diagram) (Flemming, 2000). For instance, by taking the ratio between these three components (sand, silt, and clay), we can define and separate different types of mixtures following a traditional classification diagrams shown in Figure 3, which were developed by Shepard (1954). In mixed sediment, percentages of sand-silt-clay are used to determine cohesive and non-cohesive properties of the bed. The term called as 'critical mud/ silt content' is used to distinguish between the cohesive and non-cohesive regimes in sand-mud or sand-silt mixtures, which lead to different erosion and transport behaviors. In particular, by assuming silt/clay ratio is a constant ($p_{silt}/p_{clay} \approx 2$), the transition between non-cohesive and cohesive for sand-mud mixtures occurs at critical mud content ($p_{mud,cr}$) of 30% with clay content (p_{clay}) of 5-10% (Torfs, 1995; Van Ledden, 2003; Van Rijn, 2020). Recently, Yao et al. (2022) applied unimodal sand-silt mixtures without including clay particles ($p_{clay} \approx 0$) and found the critical silt content ($p_{silt,cr}$) of this transition is approximately 35%.

Secondly, plasticity is a property of soil when it consist of an appreciable amount of clay particles. Particularly, Plasticity Index (PI (%)) is used as a measure of plasticity property of soil. It is defined as the difference between the liquid limit (LL) and the plastic limit (PL) as: PI = LL – PL. The liquid sslimit is the gravimetric water content ($W = m_w/m_s$, with m_w and m_s the mass of water and solids in the bed, respectively) at the transition from plastic behavior (soil can deform without breaking) to liquid behavior (as a thick fluid), while the plastic limit is the water content at the transition from solid to plastic behavior. Higher PI values generally correspond to soils with high clay content, while PI = 0 signifies non-plastic soils with little or no clay. Notably, PI < 7 for slightly plastic soils, $7 \leq \text{PI} \leq 17$ is the range for medium plastic soils and PI > 17 shows highly plastic soils (Jacobs et al., 2011; Van Rijn, 2020).

Thirdly, bulk density, which is the mass of sediment per unit volume, indicates how densely or loosely packed a sediment bed is. There are two types: the wet and dry bulk density that can be calculated in the following way:

$$\rho_{b,dry} = \frac{M_s}{V_{tot}} = \rho_s \frac{V_s}{V_{tot}} = \rho_s \frac{(V_{tot} - V_w)}{V_{tot}} = \rho_s(1 - \eta) \tag{3.1}$$

$$\rho_{b,wet} = \frac{M_{tot}}{V_{tot}} = \frac{M_s + M_w}{V_{tot}} = \rho_w \eta + \rho_s(1 - \eta) \tag{3.2}$$

where M_s is sediment mass in soil; M_w is water mass in soil; $M_{tot} = M_s + M_w$ is total soil mass; V_s is sediment volume in soil; V_w is water volume in soil; V_{tot} is total volume of soil; ρ_s is sediment density; ρ_w is water density; $\eta = \frac{V_w}{V_{tot}}$ is porosity. Higher bulk density means a decrease in the water content within the bed, or a reduction in the distance between particles, thereby increasing the Van der Waals forces between particles and enhancing cohesion of the bed.

Muddy beds have a lower bulk density compared to sandy beds because the finer particles in mud create smaller pores, which help to contain more water. Besides, organic matters in muddy environment can form flakes with a more open structure which can content more water. However, over time, due to gravitation pores water can be expelled out of the bed and particles can come closer and stick together. This time-dependent process is called consolidation and takes longer time (days to weeks) for very fine grains (clays) (Torfs et al., 1996; Van Ledden, 2003; Van Rijn, 2020; Winterwerp et al., 2021). Consolidation is typically associated with clay-dominated beds, where a space-filling network is formed by cohesive sediment flocs (aggregates formed by the adhesion of very fine cohesive particles, such as clay). Silt, in contrast, does not form flocs and therefore follows a different mechanism. This compression process typically occurs more quickly (within a few hours) and is referred to as “compaction” in most

studies on sand-silt mixtures (te Slaa, 2020; Yao et al., 2022). Because silt does not flocculate, permeability (i.e., a measure of how easily water can flow in and out of the bed) is the primary factor affecting compaction and bulk density in sand-silt mixed beds. Fine-grained beds have smaller voids, therefore, usually have lower permeability compared to coarse-grained beds. Overall, compaction/consolidation can increase bulk density and enhance the stability of the bed. Roberts et al. (1998) found that erosion threshold of small particles (D < 220 μm) has a strong dependency on bulk density, whereas it is independent for coarser grains. This relationship will be discussed more detailed in section 4.2.

In mixed sediment, fine particles (clay and silt) can fill in sand pores instead of water. An increase of fine-grained contents can reduce the permeability of the bed and increase the bulk density. This lower permeability can slow down porewater flows and enhance bed stability (Mohr et al., 2018; te Slaa, 2020; Yao et al., 2022). Especially in bimodal sand-silt mixtures which have large grain-size ratio ($RD = D_{sand}/D_{silt}$ = 5.5 and 7.7 in studies of Bartzke et al. (2013) and Staudt et al. (2019), respectively), silt particles can fill in the large voids between sand particles causing an increase bed stability which they called “pore-space blocking” phenomenon.

3.3 NETWORK STRUCTURE

Besides cohesion, the network structure (i.e., packing status) of sediment particles affects the stability of mixed beds. For pure sands, Van Ledden (2003) stated that when the volume content of sand exceeds the critical volume of space (40-50%), sand particles begin to contact surrounding particles and form a network structure. If the volume content of water increases (i.e., more water in the bed), sand particles become looser due to the increased distances between them. If the water exceeds the critical volume of space, the sand-water mixture can flow quickly like a fluid. Silt particles start forming a network structure if their volume fraction exceeds 43% (te Slaa, 2020 In mixed sediments, the pore volume between sand particles can be occupied by finer particles (such as silt and clay) instead of water. Therefore, the network structure is also a function of bulk density, and compaction/consolidation processes directly impact this parameter. Similar to section 3.2, a denser bed (where water particles are expelled and fine particles fill in due to compaction/consolidation) reduces the distance between sediment particles, thus facilitating network structure formation. For sand-mud mixtures, network structure is built by sand particles and muddy aggregates. Figure 4 illustrates the network structures of two types of sand-mud mixtures: non-cohesive and cohesive mixtures. In particular, in non-cohesive mixtures ($p_{mud} < 30\%$), sand is “only” covered by a skin layer of cohesive particles, whereas in cohesive mixtures ($p_{mud} \geq 30\%$), sand particle is drowned into mud particles. In silty environments, the bed

network structure is formed mainly by the interaction between the sand and silt particles in which fine particles can fill in coarse pores and stabilizing the bed. However, there is not yet a study mentioned clearly about the network structure of non-cohesive or cohesive sand-silt mixtures.

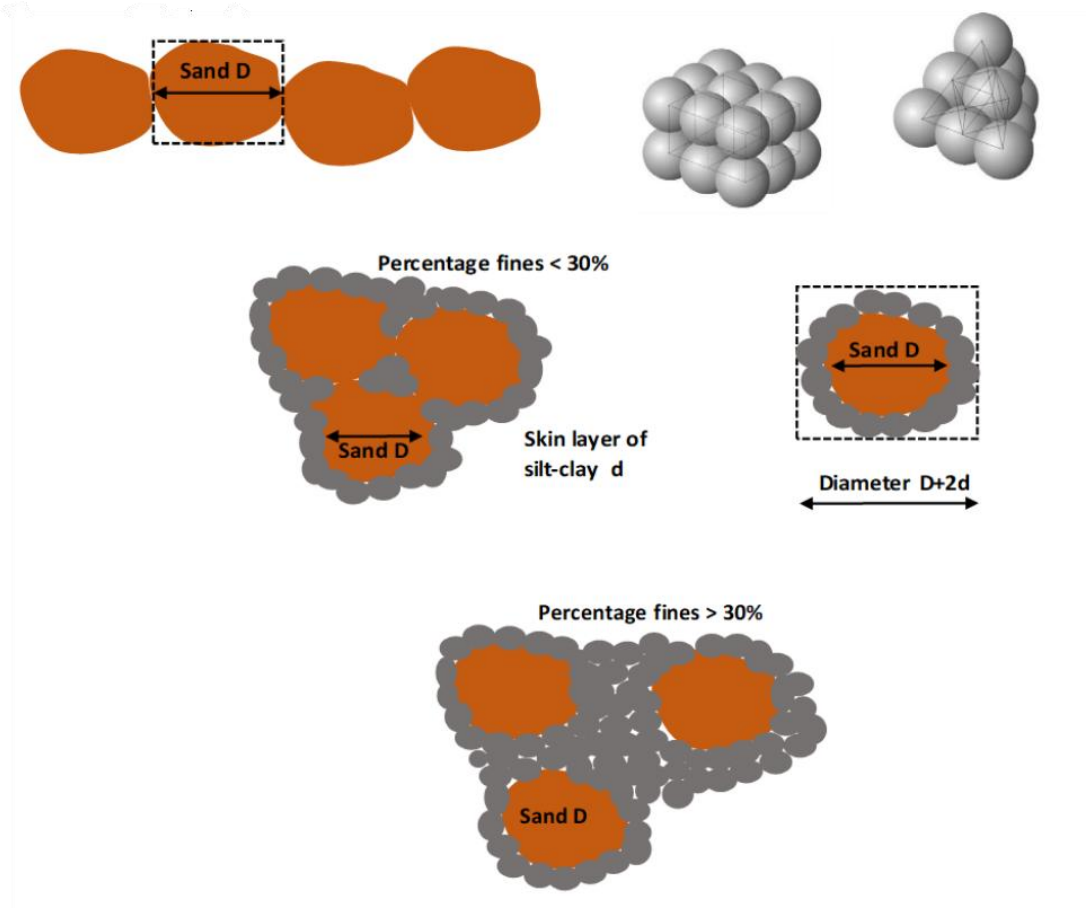

Figure 4. Network structure of sand-mud mixtures. There are structures of pure sand, sand particle with a skin layer of mud (mud content < 30%) and sand particles surrounded by a thick layer of mud (mud content > 30%) from top to bottom, respectively. (Van Rijn, 2020)

4. PHYSICAL PROCESSES OF SAND-MUD MIXTURES

4.1 BED-SHEAR STRESS

Bed-shear stress (τ_b) is a fundamental concept representing the force of water flows (waves and currents) on the sediment bed and driving the erosion, transport, and deposition of sediment particles. For practical purposes, bed-shear stress is commonly related to a parameter called as friction/ shear velocity (u_*) as $\tau_b = \rho_w u_*^2$. Even though using as a velocity scale, friction velocity does not correspond to a real flow velocity. The bed-shear stress primarily depends on vertical velocity gradient (shear) as follows:

$$\tau_b = \rho_w \nu \frac{\partial u}{\partial z} \tag{4.1}$$

where ρ_w is water density; ν is kinematic viscosity and $\frac{\partial u}{\partial z}$ and $\frac{\partial u}{\partial z}$ is vertical gradient of velocity u. The flow layer which is influenced by friction of the bed is called as the "bottom boundary layer" (BBL). In fully-developed turbulent flows (steady and horizontally uniform), velocity profile in BBL can be described as logarithmic profile:

$$u(z) = \frac{u_*}{\kappa} \ln\left(\frac{z}{z_0}\right) \tag{4.2}$$

with $\kappa = 0.4$ is a Von Karmann constant; $z_0 = \frac{k_s}{30}$ is roughness length (or hydraulic roughness) which is the height above the bed where velocity equals zero and $k_s = 2.5D_{50}$ is the Nikuradse roughness height which is strongly dependent on grain size. Roughness height is lower or bed surface is smoother for smaller grain sizes. In bimodal sand-silt mixtures, fine silt particles with higher *RD* can fill in more between sand pores lead to smoother bed surface and enhance near-bed velocity (Staudt et al., 2017).

Besides, bed shear stress can also be represented in a non-dimensional way using the Shields number (or Shields parameter) as follows:

$$\theta = \frac{\tau_b}{(\rho_s - \rho_w) g D} \tag{4.3}$$

Shields numebr quantifies the ratio between the forces moving the particles (such as fluid drag and lift) and the forces resisting the motion (mainly due to the weight of the particles). Therefore, Shields number is usually used to describe the initiation of motion for sediment particles on a bed due to fluid flow.

In coastal areas, waves and currents are two types of flows commonly considered. A simple bed-shear stress induced by currents can be expressed as (Van Rijn, 1993):

$$\tau_{b,c} = \rho_w g \left(\frac{\overline{u_c}}{C}\right)^2 = 0.125 \rho_w f_c (\overline{u_c})^2 \tag{4.4}$$

with g is gravity acceleration; $\overline{u_c}$ is depth-averaged current velocity; $f_c = 8g/C^2$ is friction coefficient induced by currents; $C = 5.75g^{0.5}\log(12h/k_s)$ is Chézy coefficient for rough flow conditions; h is water depth.

The average bed-shear stress induced by maximum orbital velocity over the wave cycle is given by:

$$\tau_{b,w,m} = 0.5\,\rho_w f_w (U_{max})^2 \tag{4.5}$$

with $f_w = 0.00251\exp[5.21(A_{max}/k_s)^{-0.19}]$ for $A_{max}/k_s > 1.57$ and $f_w = 0.3$ for $A_{max}/k_s \leq 1.57$ is the wave friction coefficient for rough conditions; $U_{max} = \pi H/[T\sinh(kh)]$ is maximum orbital velocity near the bed (right above wave boundary layer) based on linear wave theory; H is wave height; T is wave period; h is water depth; $k = 2\pi/L$ is wave number; A_{max} is maximum orbital excursion ($U_{max} = 2\pi A_{max}/T$); L is wave length.

The combination of two bed-shear stresses of wave and current cannot be calculated by addition of wave-only and current-only bed-shear stress because of the non-linear interaction of wave and current boundary layer. The bed-shear stress can be calculated by relating the instantaneous total bed-shear stress to an instantaneous near-bed velocity (u_{nb}) :

$$\tau_{b,wc}(t) = \frac{1}{2}\rho_w f_{wc}|u_{nb}(t)|u_{nb}(t) \tag{4.6}$$

with $f_{wc} = \alpha_{wc} f_c + (1 - \alpha_{wc})$ is the wave-current friction factor with $\alpha_{wc} = \frac{\langle u_b \rangle}{\langle u_b \rangle + U_w}$ is the relative current strength and u_b is the current velocity at the near-bed level.

4.2 EROSION OF MIXED-SEDIMENT BEDS

Sediment particles and flocs on bed surface are eroded (detached) from the bed when the combined wave-current bed shear stresses (τ_b) exceed the critical bed shear stress (τ_{cr}) which is also known as the erosion threshold. This erosion threshold primarily depends on properties (cohesive or non-cohesive, density, composition) of materials and network structure of the bed. Non-cohesive bed (sand) do not form a coherent mass due to inert property and assumed granular structure of particles. Therefore, particle size and weight are important parameters for erosion. In contrast, cohesive particles (very fine silt and clay) stick together by molecular force or hydrogen bond between particles forming a coherent mass. Thus, these cohesive properties dominate the erosion behaviors while the particles size and weight have a minor contribution.

Many experiments demonstrate a higher erosion threshold when adding a little mud to a sand bed (Mitchener and Torfs, 1996; Barry et al., 2006) or vice versa (Williamson and Ockenden, 1993) compared to pure-sand beds. Mitchener and Torfs (1996) found that erosion rate decreases and critical bed shear stress increases when adding sand to mud bed or vice versa by examining the erosion behavior of sand-mud mixtures using both of laboratory and field data. Particularly, the critical shear stress for erosion increased by factor of 2 for addition up to 50% of sand to muddy beds while it can reach to a factor of 10 when adding 30% of mud to sandy beds. Behaviors of the mixed sediment is similar to mud if mud content is larger than 50%. Panagiotopoulos et al. (1997) found that erosion threshold is significantly higher for mud content ranging from 30 – 50% by testing erosion threshold of sand – mud mixtures under both unidirectional current and simulated wave. They stated that the sediment transiting started to show cohesive behavior at a clay content of 5 – 10%. Perera et al. (2020) found that the critical bed shear stress increased by a factor of 2 to 3 compared to the non-cohesive (sand) bed with 8% mud content, reaching a maximum at 30-40% mud content with the mud content increased from 0% to 100%.

In general, the critical bed shear stress was found to significantly increase until reaching a critical mud/silt content and remained nearly consistent until pure-mud regime. This critical mud/ silt content is also the parameter to distinguish non-cohesive and cohesive regimes of mixed sediment beds (please see section 3.2). The critical mud content is commonly defined as 30% including 10% of clay content based on experimental studies (Mitchener and Torfs, 1996; Panagiotopoulos et al., 1997; Barry et al., 2006; Jacobs et al., 2011; Perera et al., 2020) and widely applied in sand-mud mixtures studies (Van Ledden, 2003; Van Rijn, 2020; Colina Alonso et al., 2023). Differently from sand-mud mixtures, sand-silt mixtures which has weaker cohesion certainly have lower erosion thresholds (please see Figure 6 in chapter 5). However, sand-silt mixtures have nearly similar trend when critical bed shear stress also increases until critical silt content and remain practically consistent for higher silt contents. Critical silt content for unimodal sand-silt mixtures was recently found as 35% by Yao et al. (2022).

Besides the cohesive effect, the packing of the bed (network structure) also affects the erosion process, especially for bimodal sand-silt mixtures. Even though there is no cohesive fraction when using coarse silt ($D_{50,silt}$ = 55 μm) mixed with medium sand ($D_{50,sand}$ = 300 μm), Bartzke et al. (2013) found critical silt content of less than 1%, This is due to the “pore-space blocking” effect. As mentioned in Section 3.2, fine particles (silts) can fill the pores of coarse particles which makes the bed more packed and enhance bed stability. Staudt et al. (2017, 2019) tested multiple bimodal sand-silt mixtures and found that if the grain-size ratio is large enough (RD > 4-5), the bed is more stable compare to unimodal mixtures. In contrast, when the ratio is smaller (RD <

3.5), the pore-spaces between fine sand are too limited for fine grains to percolate inside, which results in sand-like erosion behavior. Figure 5 shows a similar trend of bed mobility as a function of *RD* but natural sand-silt mixtures have a lower bed mobility compared to glass beads. This is caused by the angular shape of natural sediments which leads to higher intergranular friction compared to the more smooth spherical beads beds. If filling-pores is considered the micro-scale effect, the increase in bulk density due to fine particles percolate into coarse pores can be seen as the macro-scale effect. Denser beds (or high-bulk-density beds) have lower permeability (i.e. water hardly infiltrate into sediment bed). Therefore, it is more difficult for water flows to erode sediment particles.

Furthermore, on the bed surface, fine particles can hide among coarse particle (or coarse particles are more exposed to the flow). This is called hiding-exposure effect and it results in an increased mobility of coarse particles and decreases mobility of finer grains. The hiding-exposure effect is usually applied for gravel-sand beds (for more information see McCarron et al. (2018)). However, recent observations of increased dune heights and lengths of sand-silt mixtures in an experimental study of de Lange et al. (2024) showed parallel results to gravel-sand mixtures as a smaller scale. The hiding-

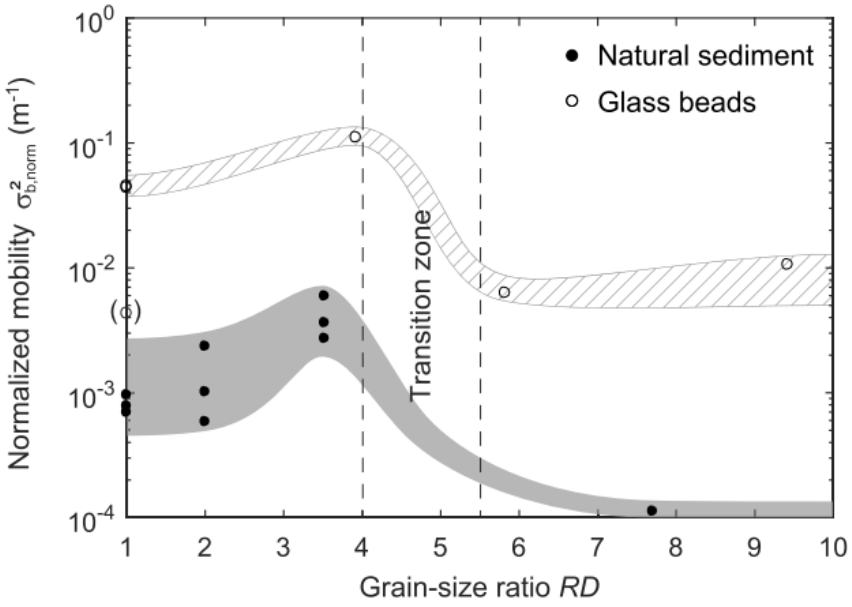

Figure 5. Normalized mobility, i.e. variance of the bottom level (logarithmic scale), with varying grain-size ratio. Values for natural sediment and glass beads are shown in filled and open circles, respectively. The shaded grey and striped areas indicate the proposed trend of mobility with changing RD for natural and artificial sediment. The value in brackets is regarded as an outlier, as the glass beads were not remixed properly before this experiment (figure taken from Staudt et al. (2019)).

exposure effect mainly depends on *RD*. De Lange et al. distinguished three regime: (1) $RD < 2$: no biased mobilization of coarse grains; (2): $2 < RD < 20$: fine particles are small enough to fill in pores and hide between coarse-grained matrix causing an increased mobility of coarse grains; (3): $RD > 20$: fines percolate into sublayer of coarse-grain matrix and do not appear in surface layer because they are transported away in suspension (for further review and discussion on hiding-exposure effect, see de Lange et al. (2024)).

For cohesive sand-mud mixtures, there are three main erosion types following Winterwerp et al. (2021):

- Floc erosion: some individual particles and small flocs from the fluffy top layer of the bed surface are picked during part of time.
- Surface erosion: with increasing flow velocities, the bed-shear stress is large enough to easily break the bonds of particles network structure in drained condition. Thereby, several layers of particles on the surface are torn from the bed concurrently with the continuity of floc erosion (left panel of Figure 6).
- Mass erosion: when the bed-shear stresses induced by flows are larger than the local undrain shear strength of soil, which is the maximum shear stress a soil can sustain without a change in its water content, large lumps of sediment can be eroded from the bed (right panel of Figure 6).

However, it the erosion behaviors of sand-silt mixtures is still unclear. For instance, Staudt et al. (2019) found that silt particles are washed out through pores of the sandy bed and separately transported in suspension as non-cohesive sediments. This was evidenced by observations of an increase in suspended sediment concentration (SSC) at relatively low velocities, while the bed remained flat throughout the experiment. In other studies mass erosion was observed for sand-silt mixtures consisting very fine silts that approach the clay regime (Zuo et al., 2017; te Slaa, 2020). Furthermore, the critical silt content for unimodal and bimodal sand-silt mixtures is still not well understood. Particularly, due to packing effect (large *RD*), the critical silt content of bimodal mixed

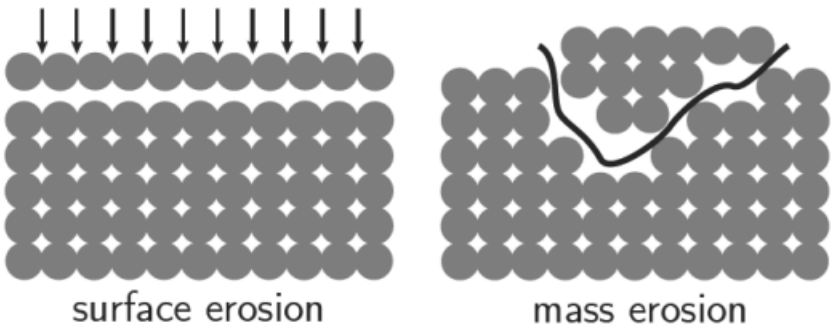

Figure 6. Sketch of surface erosion and mass erosion (Winterwerp et al., 2021)

beds can be much smaller (p_{silt} ~ 0.18% followed by Bartzke et al. (2013)) than unimodal beds (p_{silt} ~ 35% following Yao et al. (2022)). Besides, hiding-exposure effects on erosion of sand-silt mixtures are still not well-understood (de Lange et al., 2024).

4.3 TRANSPORT OF MIXED SEDIMENTS

After being eroded from the bed when bed shear stress of the flow exceeds the erosion threshold, particles start moving as bedload. This involves rolling, sliding and saltation of grains along the bed. Sediment particles are frequently in contact with the bed and each other; intergranular forces are important. For stronger flows and/or finer particles sizes, sediment is entrained off the bed and carried with the flow velocity as suspended load. As a result, the relative importance of bedload and suspended depends on the sediment grain size. Generally sand is transported as both bedload and suspended load, and clay as suspended load. The prevailing transport mode of silt is generally suspended load, although bedload may take place at low flow velocities (Van Rijn, 2020; Colina Alonso et al., 2023).

In coastal areas, two main components contributing to sediment transport are waves and currents. Waves mainly stir the bed sediments and make it suspended into water column with oscillatory motions. However, for non-linear waves in shallow water region, waves deform having higher but short wave crests and longer but less deep wave troughs in shallow water (wave skewness). This results in relative higher onshore near-bed velocity peaks (velocity skewness) which can generate a net (wave-averaged) transport sediment in the on-shore direction. This wave-related transport is applicable for sand which has settling velocity of ~cm/s because the velocity peaks coincide with relative high pulses of sand concentration. In contrast, clay particles having settling velocity is quite small (~ mm/s) due to their small size leading to the phase coupling between orbital velocities and sediment concentrations is generally absent. Therefore, wave-related suspended transport is negligible for clays.

Besides, there is another principle difference between transport of sand and clays. Due to the cohesionless and larger size, erosion from the bed and deposition from the water column are relatively balance for sand particles. Therefore, the carrying capacity of the flow controls the amount of sand transport, i.e. stronger flows lead to larger transport rates. Conversely, due to cohesive effects, the supply of muddy/ clayed beds from the bed is limited and the transport carrying capacity of the flow is not reached. Thus, in muddy cases, the erosion from the bed controls the amount of mud transport, i.e. higher erosion rates lead to larger transport rates (Winterwerp et al., 2021).

In sand-mud mixtures, transport of sand and mud fractions are defined following cohesive characteristics of the bed which is determined by using critical mud content

value (Van Ledden, 2003). In non-cohesive regime ($p_{mud} < p_{mud,cr}$), sand is dominant and mud/fines are washed out proportional to sand. Conversely, erosion and pick-up process of sand from the bed is limited by cohesion caused by fines particles if mud content exceeds the critical mud content. Hence, mud transport is dominated in the cohesive regime and sand is eroded proportional to the mud (Van Ledden, 2003). Furthermore, the absence of ripples during experiments with cohesive sand-mud mixtures (Mitchener and Torfs, 1996; Panagiotopoulos et al., 1997; Van Ledden, 2003), i.e. bed load transport of sand is not possible and assumed equals zero. Hence, sand is assumed to be transported in suspension only with mud aggregations in cohesive sand-mud mixtures (Van Ledden, 2003).

In sand-silt mixtures, many experimental studies found that silt particles can be washed out through pores of the sandy bed and separately transported in suspension as non-cohesive sediment (Staudt et al., 2019; Yao et al., 2022). These suspended silt particles left coarse sand at the bed surface forming ripples which indicated for bedload transport of sand particles. In particular, Yao et al. (2022) found ripples for most of mixtures except of mixtures with 60% of silt content.

5. MIXED SEDIMENT LABORATORY EXPERIMENTS

As mentioned in chapter 4, studies about cohesive-mixed sediment commonly care of erosion process due to erosions control transport amount of sediments. Therefore, there have been many experiments (both in the laboratory and field) carried out to study about erosion of mixed sediments. Most laboratory experiments were conducted to determine erosion thresholds as well as erosion rates of sand-mud/sand-silt mixtures. For non-cohesive sediment (sands), incipient motion is determined visually through four stages: (1): movement of single particles at some locations; (2): frequent movement of 10% of sediment surface; (3): movement of 50% sediment surface at many locations; (4) movement of all particles (100% of sediment surface) at all locations (Van Rijn, 2020). However, this visual method is challenging for fine sediments (Panagiotopoulos et al., 1997; Yao et al., 2022). Therefore, another method involves using either a critical erosion rate (critical bed shear stress and erosion rate threshold; erosion rates can be measured relatively accurately) or a critical SSC (the point at which the suspended sediment concentrations increase rapidly as indicator of bed erosion) (Roberts et al., 1998; Mohr et al., 2018; Staudt et al., 2019; Yao et al., 2022). Nevertheless, there is no consistent value for either the critical erosion rate or critical SSC to establish the erosion threshold (Yao et al., 2022). In experiments, SSC and flow velocity can be measured by optical and acoustic instruments, e.g. using OBS and ADV, ADVP. The erosion rate is determined by the estimated eroded sediment mass and the time elapsed.

5.1 SAND-MUD EXPERIMENTS

Mitchener and Torfs (1996) examine the erosion behavior of sand-mud mixtures using both of laboratory and field data which include artificial and undisturbed-natural mixtures, respectively. Regarding laboratory experiments, they tested in different flume consisting of straight unidirectional flumes, annular flumes and wave flumes.

Panagiotopoulos et al. (1997) is also one of few studies tested the erosion threshold of sand-mud mixtures under both unidirectional current (mean critical speeds ranging from 0.124 – 0.182 m/s) and simulated wave (mean critical period ranging from 2 – 6.7 s with near-bed amplitudes of 0.28 – 0.57 m). The experiments were carried out in a a recirculating (Armfield) flume (5.00 m long, 0.30 m wide and 0.45 m deep), with an open top and glass-sided walls. Two sand sizes (152.5 and 215 μm) were mixed with separately with mud with various proportions, i.e. 5%, lo%, 20%, 30%, 40% and 50%, by dry weight.

Le Hir et al. (2005) studied erodibility of sand-mud mixtures in a re-circulating small-scale rectangular flume so called “Erodimetre” (length=1.2m, width=0.08 m, height=0.02 m). There were several sand-mud mixtures created by mixing natural muds

from the Penzé estuary and Bay of Brest (France) with two sand fractions (D_{50} = 140 and 280 μm) and the natural mixed sediment from Mont St-Michel Bay (France).

Jacobs et al. (2011) did a large number of erosion tests (about 50) with artificially generated sand-mud mixtures in the same "Erodimetre" flume. The sediment cores were placed in a sediment tray at the bottom of the flume and pushed upward for erosion tests under unidirectional flow conditions. There was a sand trap at the downstream to collect the eroded sediment at the end of each velocity step. After experiments, they found some cracks in the test section including both of radial cracks (mostly) and cracks parallel to the flow direction on the surface of clay-dominated sediment samples.

Perera et al. (2020) studied the erosion of sand mixed with kaolinite, kaolinite-bentonite, and Mississippi River muds under unidirectional flow conditions using a small-scale SEDFlume (1 m length, 0.1 m width, and 0.02 m depth) (Figure 15). As the mud content increased from 0% to 100%, they found that the critical bed shear stress increased by a factor of 2 to 3 compared to the non-cohesive (sand) bed with 8% mud content, reaching a maximum at 30-40% mud content. This trend was consistent for all three types of mud. Conversely, a ten- to one hundredfold decrease in erosion rate was observed with as little as 5% mud content, reaching a minimum at 30-40% mud content.

More recently, Van Rijn et al. (2020) carried out experiments in a flume (5 m long, 0.3 m wide and high) and propeller-operated tube (Eromes-tube) to study erosion of sand-mud mixtures collected from the field (e.g. Noordpolderzijl and Western Scheldt Estuary (Netherlands), Plymouth Estuary (United Kingdom)). This project is also known as MUSA 1. Three erosion types: particle/ floc erosion, surface erosion and mass erosion, were observed visually via experiments. Clay content in collected samples at Western Scheldt Estuary in range of 10% in sandy areas to more than 50% in very muddy areas.

In conclusion, there were many studies have been conducted to enhance the understanding about erosion behaviors of sand-mud mixtures including lab and field experiments. In the lab, there were many experiments were conducted mostly under unidirectional flows, some in wave-related and wave-current combined conditions. Sand-mud mixtures were mixed in various proportions from 0% to 100% in very controlled and accurate methods.

Table 3 summarizes existing lab data of the critical bed-shear stress sand- mud mixtures (taken from Van Rijn et al. , 2020). Most studies considered the erosion of sand – mud mixtures under unidirectional flow or current-only condition. There are only a few studies that tested with sand-mud mixtures under wave or wave-current interactions. This limitation may be due to the cohesive sediment usually exist in low-energy environments where wave action is not significant and the current's role is dominant in sediment transport.

Table 3. Critical bed-shear stress for erosion of mud-sand mixtures without biogenic effects; literature data (Van Rijn, 2020).

Type of mud-sand mixture	Percentage of mud (< 63μm)	Mean sediment size d_{50} (μm)	Dry bulk density top layer (kg/m^3)	Critical bed-shear stress for particle (p.e.) and surface (s.e.) of sand and mud fraction (N/m^2)
Laboratory flume (Jacobs 2011)	10%	100-150	>1800	0.18 ± 0.04 (p.e./s.e.)
	25%	80-100	>1800	0.5 ± 0.15 (p.e./s.e.)
	55%	60-80	>1800	0.7 ± 0.3 (p.e./s.e.)
	80%	30-60	>1800	1 ± 0.4 (p.e./s.e.)
Lab and field (Le Hir et al. 2008)	20%	<140	>1500	0.25 ± 0.05 (p.e./s.e.)
	30%	<140	>1500	0.4 ± 0.1 (p.e./s.e.)
	40%	<140	>1500	0.6 ± 0.15 (p.e./s.e.)
	60%	<140	>1500	1.1 ± 0.3 (p.e./s.e.)
	70%	<140	>1500	1.5 ± 0.4 (p.e./s.e.)
	90%	<140	>1500	2.0 ± 0.5 (p.e./s.e.)
Lab and field (Mitchener-Torf 1996)	>70%	<63	400	0.2 ± 0.1 (p.e./s.e.)
	40%	<100	800	0.6 ± 0.3 (p.e./s.e.)
	30%	<100	1000	1.0 ± 0.4 (p.e./s.e.)
Dutch Wadden Sea intertidal flats (Houwing 2000)	<10%	100-150	> 1000	0.1-0.2 (p.e.)
	15%-20%	100-150	> 1000	0.1-0.2 (p.e.)
	35%	50-100	> 1000	>0.5 (p.e.)

Dutch Wadden Sea subtidal channel Holwerd (Deltares 2016)	70%	20-50	300-500	0.2-0.25 mud fraction 0.3-0.35 sand Fraction (s.e)
Dutch North Sea bed (subtidal) (Deltares/ Delft Hydraulics 1989)	0-30%	100-150	> 800	0.2-0.4 (p.e.)
	50%	50-100	> 800	0.6-1.0 (p.e.)
German Wadden Sea intertidal flats (Tolhurst et al. 2000)	15%-30%	100-150	> 1000	0.2-0.5 (p.e.)
	40%-50%	50-100	>800	0.2-0.5 (p.e.)
German Wadden Sea subtidal channel Nessmersiel (Bauamt 1987)	5%-30%	60-100	300-500	0.15-0.2 mud fraction (p.e.) 0.25-0.3 sand fraction (p.e.)
Lunenburg basin (subtidal), Nova Scotia, Canada (Sutherland et al. 1998)	20%-30%	30-40	<400	0.05-0.15 (p.e.)
Minas basin (subtidal), Bay of Fundy, Canada (Amos et al. 1992)	65%	20-30	>1000	0.5-1.5 (p.e.)
Tidal fraser river (intertidal), Canada (Amos et al. 1997)	65%-90%	10-20	<400	0.15-0.5 (p.e.)
Hudson Bay (subtidal), Canada (Amos et al. 1996)	40%-50%	40-60	>1000	>3.5 (p.e.)

5.2 SAND-SILT EXPERIMENTS

Besides sand-mud mixtures, there were also some experiments carried out for sand-silt mixtures (not including clays and weaker cohesion). These studies focused on sand-silt interactions (e.g. hiding-exposed effect, pore-space blocking), and how these affect erosion processes, bed mobility, bed surface roughness.

Roberts et al. (1998) applied pure-quartz particles with multiple median sizes ranging from 5.7 to 1,350 μm to observe the effect of particle size and bulk density on the erosion process. To test with different bulk densities, they let sediment beds be compacted from 8 hours to 124 days before running experiments in a straight flume.

Bartzke et al. (2013) applied two distinct fractions including coarse silt ($D_{50,silt}$ = 55 μm) from Waikareao Estuary, Tauranga Harbor (New Zealand) and medium sand ($D_{50,sand}$ = 300 μm) from Pauanui Beach (New Zealand). The experiments were conducted in an annular flume to test the transport and stability of sand-silt-mixed beds. They tested with two bed conditions: (1) layered-bed experiment, in which a 10-cm-layered sandy bed was covered by a thin layer (0.2–3 mm) of silt with p_{silt}= 0.5– 3.7% (dry weight), and (2) mixed-bed experiment, where the bed was composed of a fully mixed sand-silt bed (p_{silt} = 0.07– 0.7%, dry weight).

Yao et al. (2015) conducted laboratory experiments to observe the erosion of two in-situ mixtures: a silt-size mixture (D_{50} = 46 μm) and a fine sand-size mixture (D_{50} = 88 μm) in a wave-current flume. They tested under both wave-only and wave-current combination conditions, in which the current directions followed and opposed the wave direction. Through experiments, they observed a high concentration layer near the bottom with a higher silt concentration in silty mixtures and bedform development of both mixtures in wave-only conditions.

Zuo et al. (2017) is another study that carried out experiments using sand-silt mixtures under combinations of waves and bidirectional currents in a wave-current flume. The flume is 175 m long, 1.6 m wide, and 1.2 m deep. They used two sediment samples, including fine (D_{50} = 68 μm) and coarse (D_{50} = 125 μm), representing silt and sand, respectively. The sediment test section was 10 m long and 0.1 m thick.

Staudt et al. (2017) studied the role of grain-size ratio (*RD*) on bed mobility by applying glass beads (a spherical and well-sorted material which has main composition is silica (SiO_2) and density of 2500 kg/m^3). By mixing 40% of very-fine-sand-sized (93, 63 μm) and silt-sized (39 μm) fractions with coarse-sand-sized (367 μm) fraction, they created three different *RD* (3.9, 5.8 and 9.4). They observed that fine particles filled in pores of coarse grain matrix leads to smoother bed surface (reduce bed roughness) and increase near-bed velocity.

Yao et al. (2018) conducted experiments in an annular flume with two sand-silt mixtures were re-mixed by sediment samples collected from silt-dominated tidal flat (middle Jiangsu coast, China). These two unimodal mixtures (*RD* ~ 2.2) have median grain size of 82 μm and 52 μm according to silt percentages of 30% and 60%, respectively. After testing in a annular flume, they found that the critical bed shear stress for erosion for the 60%-silt-content bed (0.21 N/m^2) is double compared to the 30%-silt-content bed (0.09 N/m^2).

After glass-beads experiment, Staudt et al. (2019) continued with another experiments with natural sediment collected from Waikato coast (New Zealand). By keeping same fines contents (40%) and testing in an annular flume as previous experiment, they found a similar trend of bed mobility as a function of *RD* but natural

sand-silt mixtures have lower values compared to glass beads. This is caused by angular shape of natural sediments which has higher intergranular friction compared to smoothly spherical beads beds.

te Slaa (2020) tested two groups of silty samples: Group (1) includes two deposited pure silt beds taken from laboratory and Group (2) consists of two silt-rich samples collected from the North Eastern mudflat of Chongming Island (Yangtze River Estuary, China). Erosion thresholds of natural silt-rich samples were found higher (0.25 – 0.3 Pa) compared to pure-silt beds (0.1 – 0.15 Pa). This is because natural silty sediments were close to the clay regime when containing nearly 10% of clay leading to a relatively small median grain size (D_{50} ~ 12 μm).

After the previous experiment with only two sand-silt mixtures, Yao et al. (2022) conducted another erosion experiment on sand-silt mixtures in the same annular flume, but with a wider and more detailed range of silt contents (19% - 78%). Similarly, they continued to apply unimodal-distributional sand-silt mixtures (RD ~ 2.0) collected from the Tiaozini tidal flat at the central Jiangsu coast, China. With more proportions of sand-silt mixtures, they found critical shear stress for erosion significantly increase and reached a maximum at 36% of silt content after which it remained more or less constant.

de Lange et al. (2024) carried out a laboratory experiment in a recirculating flume to study bedform developments of sand-silt mixtures. Particularly, there were three groups of mixtures created by mixing a base sediment of medium sand (D_{50} = 256 μm) with fine sand (D_{50} = 170 μm), coarse silt (D_{50} = 37 μm) and fine silt (D_{50} = 17 μm) corresponding to grain-size ratios of 1.5, 6.9 and 15, respectively.

The experimental studies on sand-silt mixtures are summarized in Table 4.

Generally, experimental studies on mixed sediments showed an increase of critical bed shear stresses following increasing mud contents (Figure 7). Moreover, the main difference between sand-mud and sand-silt mixtures is the clay content. In Figure 7, sand-silt mixtures in study of Yao et al. (2022) which removed much of clay-size particles generally give smaller erosion thresholds compared to other sand-mud mixtures (Le Hir et al., 2005; Jacobs et al., 2011; Perkey et al., 2020; Van Rijn, 2020).

Table 4. Laboratory experiments on erosion of silt and sand-silt mixtures

Study	**Experimental facility**	**Hydrodynamic forces**	**Sediment**	**Silt content**	**Grain-size ratio**	**Velocity (m/s)**
Bartzke et al., 2013	Annular flume	Current	Sand ($D_{50,sand}$ = 300 μm) and silt ($D_{50,silt}$ = 55 μm)	0.74 – 7.4%	5.5	0.25 – 0.3
Yao et al., 2015	Wind-wave-current flume	Wave only and wave-current combination	Sand ($D_{50,sand}$ = 88 μm) and silt ($D_{50,silt}$ = 46 μm)	26% and 68%		0.08-0.43
Zuo et al., 2017	Wave-current flume	Wave-current combination	Sand ($D_{50,sand}$ = 125 μm); silt ($D_{50,silt}$ = 68 μm)	-	-	0.08-0.23
Yao et al., 2018	Annular flume	Current	Sand ($D_{mean,sand}$ = 95-109 μm) and silt ($D_{mean,silt}$ = 45-49 μm)	30% and 60%	~ 2.2	0.17
Staudt et al., 2019	Annular flume	Current	Sand ($D_{50,sand}$ = 367; 410 μm) mixed with silt ($D_{50,silt}$ = 39; 53 μm), respectively.	40%	7.7	0.13-0.22
te Slaa, 2020	Annular flume	Current	Silt ($D_{50,silt}$ ~ 12 μm)	> 85%	-	
Yao et al., 2022	Annular flume	Current	Sand ($D_{50,sand}$ = 88 μm) and silt ($D_{50,silt}$ = 46 μm)	19 – 79%	~ 2.0	0.04-0.35
de Lange et al., 2024	Recirculating flume	Current	Medium sand ($D_{50,sand}$ = 256 μm) mixed with fine sand ($D_{50,sand}$ = 170 μm), coarse silt ($D_{50,silt}$ = 37 μm) and fine silt ($D_{50,silt}$ = 17 μm)	0-100% (fine sand) 0-51% (coarse silt) 0-30% (fine silt)	1.5 (fine sand) 6.9 (coarse silt) 15 (fine silt)	0.44

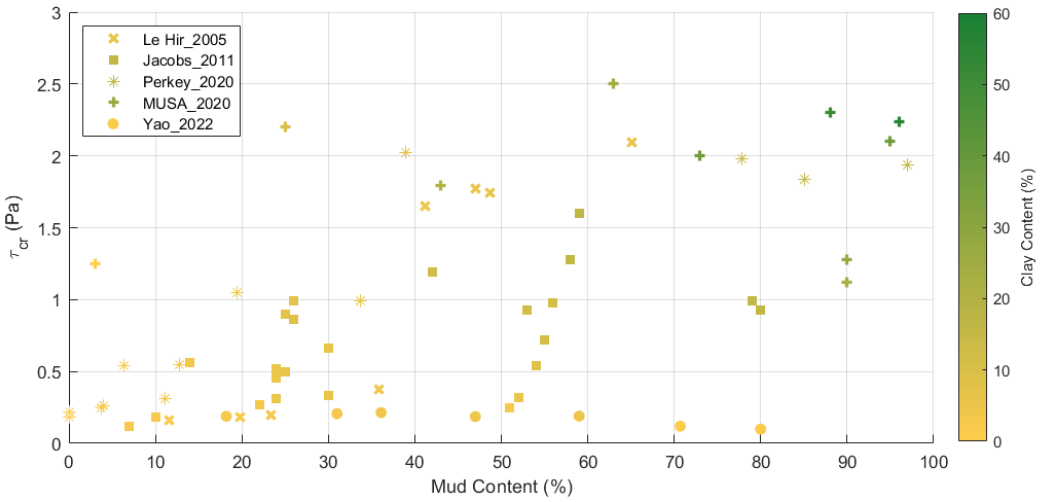

Figure 7. Measured critical bed shear stress with different mud contents in multiple experimental studies of sand-silt mixtures (Yao et al., 2022) and sand-mud mixtures (Le Hir et al., 2005; Jacobs et al., 2011; Perkey et al., 2020; Van Rijn, 2020) in which different clay contents in mixtures showed as the color bar.

6. EMPIRICAL MODELS FOR MIXED SEDIMENTS

6.1 EROSION MODELS FOR SAND-MUD MIXTURES

As discussion in section 4.2, the erosion from the bed controls the cohesive-sediment transport; i.e. larger erosion rates result into larger transport rates. Therefore, erosion models are focused and studied. A widely used is erosion formula was proposed by Van Ledden, 2003. He developed an estimation for the critical bed-shear stress for erosion of sand-mud mixtures by adding mud content into critical bed shear stress of pure-sand bed which enhances the erosion threshold. This is the critical bed shear stress in the non-cohesive regime ($p_m \leq p_{m,cr}$) where mud particles are washed out with eroded sand particles. On the other hand, by assuming bed density and silt-clay ratio are constants. critical bed shear stress of cohesive mixtures ($p_m > p_{m,cr}$) can be interpolated from the critical bed-shear stress of non-cohesive mixtures ($\tau_{sm,nc}$) and pure mud ($\tau_{e,m}$)

$$\tau_{sm,cr} =$$

$$\tau_{sm,nc} = \tau_{s,cr}(1 + p_m)^{\beta} \ ; \text{ if } p_m \leq p_{m,cr} \ (\text{non} - \text{cohesive}) \tag{6.1}$$

$$\tau_{sm,c} = \frac{\tau_{s,cr}(1+p_{m,cr})^{\beta} - \tau_{m,cr}}{1-p_{m,cr}}(1 - p_m) + \tau_{m,cr}; \text{ if } p_m > p_{m,cr} \ (\text{cohesive}) \tag{6.2}$$

where $\tau_{s,cr}$ is critical bed shear stress of pure sand; $\tau_{m,cr}$ is critical bed shear stress for pure mud; $\tau_{sm,nc}$ and $\tau_{sm,c}$ are critical bed shear stresses of non-cohesive and cohesive sand-mud mixtures, respectively; $p_{m,cr}$ is critical mud content where behavior of mixtures changing from cohesionless to cohesion; p_m is mud content in mixtures; β is an empirical coefficient ranging from 0.75 to 1.25 in study of Van Ledden, 2003 and depend on sediment packing at the bed. However, the default value of β is 3 in the Delft3D numerical modeling software (Van Ledden, 2003; Van Rijn, 2020; Colina Alonso et al., 2023).

The formulation of Van Ledden (2003) is the first formula estimating the critical shear stress for erosion of sand-mud mixtures for mud contents from 0% to 100% and is implemented in Delft3D. However, Ahmad et al. (2011) stated that we need to determine the value of critical mud content to distinguish the non-cohesive and cohesive characteristics of the sand-mud mixture which may vary depending on the specific types of mud and difficult to define. Therefore, Ahmad et al. (2011) created a new, seamless formulation to estimate critical shear stress for erosion of sand-mud mixtures. This formulation does not require the critical mud content value and only contains one coefficient (noted as β_A to distinguish from the coefficient β above in formula of Van

Ledden (2003)) depending on the type of mud and is determined by fitting with experimental data giving values of 0.1; 0.15 and 0.2 in the study of Ahmad et al., 2011.

$$\tau_{sm,cr} = e^{\beta_A\left(1-\frac{1}{p_s}\right)}\tau_{s,cr} + (1-p_s)\tau_{m,cr} \tag{6.3}$$

Also without a distinction between the non-cohesive and cohesive similar to Ahmad et al. (2011), Wu et al. (2018) give another formula which derived from a consideration of interparticle bond force induced mostly by the fine sediments. They started with consideration of the force balance including flow tractive force (F), submerged weight (W_s) of particle and interparticle bond force (T) representing for the electrochemical bonds of cohesive particles (Figure 8). They demonstrated that the critical bed-shear stress for sand-mud mixtures can be calculated as a combination of the critical shear stress of pure sand and mud as follows:

$$\tau_{sm,e} = \lambda_1\tau_{s,cr} + \lambda_2\tau_{m,cr} \tag{6.4}$$

where λ_1, λ_2 are empirical coefficients that are influenced by soil properties such as particle size, bed density, and particle voids. By applying four experimental datasets from Panagiotopoulos et al., 1997; Kothyari and Jain, 2008; Smith et al., 2015; Ye et al., 2023, they found functions for two empirical coefficients λ_1, λ_2 that lead to the final formula to calculate the critical bed-shear stress of sand-mud mixtures which can cover the entire range of mud contents (0-100%) as follows:

$$\tau_{sm,cr} = \tau_{e,L} + (\tau_{m,cr} - \tau_{e,L})\exp\left[-\alpha_w\left(\frac{p_{sand}}{p_m}\right)^{1.2}\right] \tag{6.5}$$

With $\tau_{e,L} = \tau_{s,cr} + 1.25(\tau_{m,cr} - \tau_{s,cr})\min(p_m, 0.05)$ is the critical bed-shear stress for mixtures having low mud contents; α_W is an empirical coefficient and defined as $\alpha_W = 0.42\exp(-3.38D_{50,sand})$.

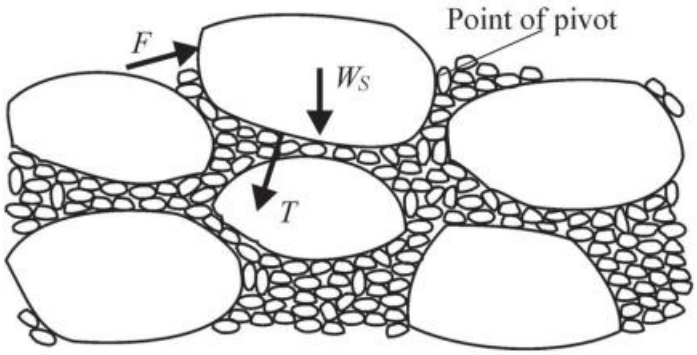

Figure 8. Forces on a sediment parcel on sand-mud beds (Wu et al., 2018)

In general, any above formula gives higher critical bed shear stress when adding mud to pure-sand beds because of cohesion forces caused mainly by clay particles. This increase of critical bed shear stress changes the erosion rate of sand-mud beds. Specifically, in the non-cohesive regime, mud particles are washed out with eroded sand particles. Therefore, by adding effect of small amount of mud content into a erosion model of Van Rijn (1993) for sandy beds, Van Ledden (2003) proposed formulas to calculate erosion rates of sands and muds in the non-cohesive regime:

$$E_{s,nc} = \frac{\alpha_{b1}}{3}\frac{\sqrt{\Delta g D_{50}}}{{D_*}^{0.9}}{T_{nc}}^{\alpha_{b2}-0.9} \tag{6.6}$$

$$E_{m,nc} = \frac{p_m}{1-p_m}\frac{\alpha_{b1}}{3}\frac{\sqrt{\Delta g D_{50}}}{{D_*}^{0.9}}{T_{nc}}^{\alpha_{b2}-0.9} \tag{6.7}$$

where $T_{nc} = \frac{\tau_b}{\tau_{s,cr}(1+p_m)^{\beta}} - 1$ is transport parameter which includes effect of small amount of mud to a non-cohesive sand-mud bed; α_{b1} and α_{b2} are coefficients depending on transport parameters T_{nc} ($\alpha_{b1} = 0.053$, $\alpha_{b2} = 2.1$ for $T_{nc} < 3$ and $\alpha_{b1} = 0.1$, $\alpha_{b2} = 1.5$ for $T_{nc} \geq 3$); $\Delta = \frac{\rho_s - \rho_w}{\rho_w}$ is the specific density; $D_* = D_{50}[(s-1)g/v^2]^{1/3}$ is dimensionless grain size. (for more details derived to formulas, please see Appendix A in Van Ledden, 2003).

On the other hand, for cohesive sand-mud beds, muds are dominant and sand particles are transported proportional to the mud fraction in the bed. Erosion rates of suspended sands and muds in cohesive sand-mud mixtures can be calculated based on formula of Partheniades, 1965 as follows:

$$E_{s,c} = (1-p_m)M_c\left(\frac{\tau_b}{\tau_{sm,c}} - 1\right)H\left(\frac{\tau_b}{\tau_{sm,c}} - 1\right) \tag{6.8}$$

$$E_{m,c} = p_m M_c\left(\frac{\tau_b}{\tau_{sm,c}} - 1\right)H\left(\frac{\tau_b}{\tau_{sm,c}} - 1\right) \tag{6.9}$$

with $H\left(\frac{\tau_b}{\tau_{c,cr}} - 1\right)$ is a Heaviside function that equals 1 when the argument is larger than 0 and equals 0 when the argument is less or equal to 0; M_c is cohesive erosion coefficient and $\log(M_c) = \frac{\log\left(\frac{M_{nc}}{1-p_{m,cr}}\right) - \log(M)}{1-p_{m,cr}}(1-p_m) + \log(M)$ with $M_{nc} = \frac{\alpha_{b1}}{3}\frac{\sqrt{\Delta g D_{50}}}{{D_*}^{0.9}}$ is non-cohesive erosion parameter; M is the erosion parameter of pure mud bed.

6.2 EROSION MODELS FOR SAND-SILT MIXTURES

Silt is still considered as non-cohesive or apparent cohesive material. Therefore, for sand-silt mixtures, many studies applied the formulas for cohesionless sediment. For a non-cohesive bed, the Shield's curve is commonly used to determine the critical shear stress as follows:

$$\frac{\tau_{s,cr}}{(\rho_s-\rho_w)gD_{50}} = 0.115(D_*)^{-0.5}, \quad \text{for } 4 \le D_* < 10 \tag{6.10}$$

$$\frac{\tau_{s,cr}}{(\rho_s-\rho_w)gD_{50}} = 0.14(D_*)^{-0.64}, \quad \text{for } 4 \le D_* < 10 \tag{6.11}$$

In which, the D_* is dimensionless grain size and $D_* = D_{50}[(s-1)g/v^2]^{1/3}$, v is the kinematic viscosity coefficient; s the relative density, $s = \rho_s/\rho_w$. This formula is suitable for natural single pear sand-dominated sand-silt mixtures according to experimental results of Yao et al., 2018. Nevertheless, above formulas have not included two important factors for fine particles such as silt and clay which are cohesion and network structure (Van Ledden et al., 2004). To apply for finer particles such as silt, the Shield's curve for silt range is modified and including cohesive effect and network structure concept as follows:

$$\tau_{ss,cr} = \frac{c_{gel}}{c_{gel,s}}\frac{D_{sand}}{D_{50}}^{\gamma} \tau_{s,cr}, \qquad \text{for } D_{50} < 62\ \mu m \tag{6.12}$$

$$\tau_{ss,cr} = (1+p_m)^3\, \tau_{s,cr}, \qquad \text{for } D_{50} \ge 62\ \mu m \tag{6.13}$$

In which, $\tau_{ss,e}$ is critical bed shear stress for sand-silt bed; c_{gel} is the gelling mass concentration of the finer particle, $c_{gel} = (D_{50}/D_{sand})c_{gel,s}$. In particular, concentration at the transition from hindered settling to consolidation process is called as the gelling concentration c_{gel} with minimum value of 120 kg/m^3 (or 0.05 as dry bulk density by volume); $c_{gel,s}$ is the dry bulk density of sand bed by mass and equals 1722 kg/m^3, or is calculated as $(1-\eta) = 0.65$ as dry bulk density by volume; η is the porosity of the sand bed ($\eta \approx 0.35$ for a pure sand bed); γ is an empirical coefficient, in range of 1-2 but the best agreement value based on experimental results is given as 1.5 (Van Rijn, 2007a). In this equation, ratio $c_{gel}/c_{gel,s}$ indicated for packing effects (or bulk density effect). Particularly for small grain size, erosion depends on bulk density while it is independent for coarser sediment (D > 222 μm) following Roberts et al. (1998). If we consider a constant bulk density by time (without compaction/ consolidation effects), smaller particles give lower bulk densities compare to coarser particles (due to higher porosity that can contain more water). Smaller particles are easier to be eroded and therefore, critical bed shear stress also decrease with decreasing

grain sizes (see packing-only function, red dashed curve in Figure 9). On the other hand, cohesive forces caused by fine particles are represented in term $(D_{sand}/D_{50})^{\gamma}$. This term show the effect of adding fine particles make smaller D_{50} of mixed bed and enhance critical bed shear stress for the bed. The formula for sand grain size is same as critical bed shear stress of non-cohesive sand-mud mixtures in section 6.1.

We know that the cohesive characteristics of mixed beds are mainly caused by clay particles (Van Ledden, 2003) and sand-silt mixtures with little or no clay content can sometimes behave like sandy beds. However, experimental study of Yao et al. (2018) showed that the Shield's curve only applies well to mixtures up to 30% silt content, while it significantly underestimates the critical bed shear stress for mixtures with 60% silt content. Even more remarkable, experimental results by Bartzke et al., 2013, using bimodal sand-silt mixtures with two distinct fractions ($D_{50,silt}$ = 55 μm and $D_{50,sand}$ = 300 μm) showed that the critical bed shear stress increased with just 0.18% of silt. This suggests that the grain-size ratio also directly impacts the bulk density and network structure of the bed (i.e., the pore-space blocking process). Further investigations into the influence of grain-size ratio on bed mobility via the network structure of bed sediments, surface roughness, and flow structure near the bed have been carried out in experimental studies by Staudt et al. (2017, 2019). However, there is still no empirical formula that has included grain-size ratio yet.

However, if the grain-size ratio is small enough (RD < 2), Yao et al. (2022) recently proposed a revised formula based on the original Shields curve by adding effect of Van der Waals force to calculate critical bed shear stress of unimodal sand-silt mixtures as follows:

$$\tau_{ss,cr} = \tau_{s,cr}\,, \qquad \text{for } D_{50} < 62\ \mu m \tag{6.14}$$

$$\tau_{ss,cr} = (1 + B_{SS})\,\tau_{s,cr}\,, \qquad \text{for } D_{50} \geq 62\ \mu m \tag{6.15}$$

where $B_{SS} = \frac{\alpha}{(s-1)gD_{50}^2}$ is a dimensionless parameter representing the effect of silt-structural force (or the Van der Waals force for cohesive sediments); $\alpha = 5.2 * 10^{-8}$ m^3/s^2 is considered as an expanded cohesive parameter obtained from experiments.

Figure 9 shows measured and calculated critical bed shear stress as a function of particle size. Particularly, measured data is taken from experimental studies focused mainly on sand-silt mixtures (te Slaa, 2020, Yao et al., 2018, 2022) or at least using uniform quartz materials (Roberts et al., 1998). Lines show calculated critical bed shear stresses using original Shields curve, Van Rijn's (2007) including cohesive and bulk density effects plotted separately and Yao's (2022) formulas. In this figure, except for the results of te Slaa (2020) including a small clay content (~ 5%), other experimental

results are closed to calculated curves using Yao's (2022) and cohesive-only equation of Van Rijn (2007). This indicates that clay content has a strong effect on the cohesive properties compared to silt particles.

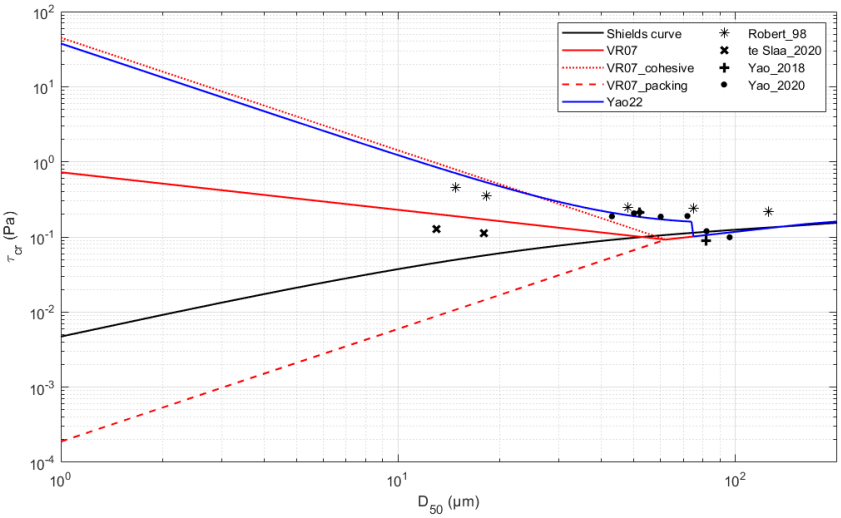

Figure 9. Measured and calculated critical bed shear stress for sand-silt mixtures as a function of median grain size

Besides of erosion thresholds, te Slaa (2020) proposed a formula to calculate surface erosion rate of sand-silt mixtures as a function of permeability, void ratio and dry density of the bed as follows:

$$E_{silt} = \alpha \frac{2\Delta k}{1+e} \rho_{dry} \frac{1}{s_u} (\tau_b - \tau_{e,silt}) \tag{6.16}$$

with α is a calibration parameter; k is permeability parameter and e is void ratio; $\tau_{e,silt}$ is the critical bed-shear stress for initial motion of fine-sediment beds and calculated following Van Rijn, 2007a equation; s_u is the undrained shear strength.

6.3 TRANSPORT MODELS FOR SAND-SILT MIXTURES

As aforementioned in section 4.3, the main difference between the transport of sand and mud (including clay) is the dependence on flow capacity and the supply limitation from the bed. Due to the small size and cohesive effects of fine particles, transport rate of muddy bed depends mainly on erosion rate in which empirical formulas were presented in section 6.1 and 6.2. In contrast, there is balance between erosion from the bed and deposition from water column for sand particles. Therefore, sand transport depends on capacity of flow which means stronger flows lead to larger transport rates. It is yet unclear what controls the transport of silt or sand-silt mixtures.

However, if we consider non-cohesive bed (p_{mud} < 30% following Van Ledden (2003)) or avoid the true cohesion effect mostly caused by clay-dominated fraction (D < 8um) in sand-silt mixtures, the mixed bed can behave as a sand bed. There are many sand transport models and be separated into four main types:

Wave-averaged models: for simplicity, wave-related transport is neglected by taking an average over wave cycles, solving only for current-related transport.

Quasi-steady models: based on the assumption that the sediment transport rate at any given moment (within a wave cycle) is a direct function of the instantaneous flow conditions (e.g., flow velocity, shear stress) without significant lag or delay.

Semi-unsteady models: These models are built as a function of both the instantaneous flow conditions and the past flow conditions to account for phase lags between the flow velocity (or shear stress) and the sediment transport rate.

Unsteady models: are firstly based on physical principles such as conversation of mass and momentum to determine sand concentration and velocity as a function of space and time.

Meyer-Peter and Müller (1948) is a well-known, relatively simple quasi-steady formula to calculate bedload transport including a critical bed shear stress for transport based on a flume experiment. Soulsby-Van Rijn models (Soulsby, 1997) is a more advanced model to calculate total load including bedload and suspended load under combination of waves and currents,. However, it does not take wave-related transport into account; wave only acts as a stirring factor (*wave-averaged model*). The bedload-transport model of Ribberink (1998) can be represented as a *quasi-steady* model in oscillatory flows where instantaneous sand transport is proportional to some power of instantaneous flow velocity but flow is assumed to be steady during a wave cycle.

The most well-known and widely-used is transport formulas provided by Van Rijn (2007a,b). This model is an example of semi-unsteady model when including phase lag effects in the model. In the first part (Van Rijn, 2007a), he gave a formular to calculate bedload under forces of wave-current combination.

$$q_b = 0.5\rho_s f_{silt} D_{50} D_*^{-0.3} \left(\frac{\tau'_{b,cw}}{\rho_w}\right)^{0.5} \left(\frac{\tau'_{b,cw} - \tau_{b,cr}}{\tau_{b,cr}}\right) \tag{6.17}$$

where $\tau'_{b,cw} = 0.5\rho_w f'_{cw}\left(U_{\delta,cw}\right)^2$ is instantaneous bed shear stress due to both waves and currents, $U_{\delta,cw}$ is instantaneous velocity of both currents and waves at edge of wave boundary layer, f'_{cw} is friction coefficient due to currents and waves; $\tau_{b,cr}$ is critical bed shear stress mentioned in section 6.3 which account for cohesion and packing effect caused by fine particles; $f_{silt} = \frac{D_{sand}}{D_{50}}$ is a silt factor. In this formula, silt effect is

accounted in critical bed shear stress and silt factor. In particular, higher silt contents give smaller D_{50} and therefore, more particles (including both sands and silts) can be picked up and transported away represented through larger f_{silt}. However, packing and cohesion effects caused by fines simultaneously can enhance critical bed shear stress, i.e. bed is more stable and obstruct bedload transport.

In second part (Van Rijn, 2007b), he described two formulas for current-related and wave-related suspended load. Firstly, the current-related transport formula is simply computed by taking vertical integration of product of wave-averaged velocity (u) and concentration profile (c) as follows:

$$q_{s,c} = \int_a^h uc\, dz \tag{6.18}$$

Where $a = \max(0.5k_{s,c}, 0.5k_{s,w})$ is the reference level and defined as maximum value of half the current-related and half the wave-related bed roughness with minimum of 0.01m. In case waves can generate suspended load due to asymmetric oscillatory flows near the bed, this is called wave-related suspended load and calculated as:

$$q_{s,w} = \gamma_w V_{skew} \int_a^\delta c\, dz \tag{6.19}$$

With

$$V_{skew} = \frac{\left(U_{on}^4 - U_{off}^4\right)}{\left(U_{on}^3 - U_{off}^3\right)} \tag{6.20}$$

is the velocity-asymmetric factor; δ is the thickness of near-bed suspension layer and $\gamma_w = 0.1$ is the phase factor; U_{on} and U_{off} are onshore-directed and offshore-directed peak orbital velocity, respectively.

Within this suspended transport model, flocculation and hindered settling effects were accounted for silt-sized particles and in salinity environments such as estuaries (*Sa* > 5 ppt, with *Sa* indicates salinity). As mentioned in section 3.2, due to cohesive properties, fine particles tend to stick together and form flocs. These flocs have larger size compared to individual particles and can increase fall velocity. Besides, suspended particles cannot settle freely in high concentration flows. This phenomena is called as hindered settling and it decrease settling velocity of particles. These two effects are accounted for through fall velocity calculations which influences the suspended concentration profiles and suspended transport directly. The suspended transport model was applied for range size from 8 to 1,000 μm. With the same velocity condition (1.5 m/s) but different salinity conditions (*Sa* = 0 ppt vs. 30 ppt), due to flocculation effect,

the peak of suspended transport was found at 8 and 62 μm, respectively. It indicated that without flocculation effect (fresh water), smaller size has higher concentration and larger suspended transport. Furthermore, in salt-water condition, concentrations decreased over the depth with decreasing size in silt range due to forming flocs in fine grain size.

7. CONCLUSION

This literature review gave an overview of the properties and transport process of sand-mud and sand-silt mixtures, i.e. in coastal environments. Four chapters were focusses on four questions, which are answered below.

Q1: What are the (physical) characteristics of coastal systems in which the beds are composed of both sand and mud?

In particular, most marine systems, especially coastal systems contain mixed sediment (e.g., estuaries, tidal basins), which can be divided into clay-dominated and silt-dominated systems. Silt-dominated systems like the Yangtze River, Yellow River, and Mekong Deltas receive significant sediment inputs from large rivers, and the spatial sediment distribution is influenced by river discharge, monsoonal winds, tidal currents and waves. On the other hand, clay-dominated systems, such as the Wadden Sea (The Netherlands), primarily receive mud from marine and fluvial sources, with fine sediments accumulating in areas with reduced wave energy.

Q2: Which physical processes control the erosion and transport of sand – mud?

Different particle sizes and mineral compositions lead to different characteristics of each sediment type as follows: sand is non-cohesive, silt is apparent cohesive and clay is cohesive. Not only cohesive properties but also interactions between these fractions (packing effect) influences the erosion and transport of mixed sediment. Particularly, many experimental studies have shown that the erosion of sand-mud and sand-silt mixtures is higher than pure sand due to cohesive properties and infilling pores induced by fine particles (silt and clay). The distinction between non-cohesive and cohesive characteristics of sand-mud/sand-silt mixtures is separated using critical mud (or silt) content. The critical mud content was defined as 30% through many experiments. On the other hand, critical silt content was defined as 35% for unimodal sand-silt mixtures but still remain uncertain for bimodal sand-silt mixtures. In sand-mud mixtures, mud is washed out with sand particles when sand is dominated in non-cohesive mixtures and vice versa, sand is transported with mud aggregates in cohesive mixtures. For sand-silt mixtures, silt is mainly transported through sand pores in suspension.

Q3: Which laboratory experiments have been carried out to study the erosion and transport of sand-mud mixtures?

There were many laboratory and field experiments tested and observed erosion of sand-mud mixtures within 50 years ago, mostly under unidirectional flow condition, but very less studies did for waves or wave-current combined conditions. To study better the characteristics and the role of each sediment fractions, samples were taken from the field but mixed artificially in the lab with accurate proportions in most of studies.

Besides, there were also studies deployed instruments directly or took cubes of sediments in the field to test in the lab. Regarding sand-silt mixtures, there were multiple laboratory experiments carried out to study initial motions, bed mobility and bedform of sand-silt mixtures recently. To distinguish from the sand-mud mixtures and avoid cohesive properties of clay fraction, most of sand-silt studies filtered very fine silt or clay particles out of samples. Similar to sand-mud studies, sands and silts were mixed artificially with accurate proportions before testing in the lab in controlled flow conditions. There were some studies used artificial materials (e.g., glass beads) with perfectly round shape to represent sand and silt fractions. However, there were very few studies observed transport of sand-silt mixtures under wave or wave-current conditions.

Q4: Which empirical formulas and models exist to compute the erosion and transport of sand-mud mixtures?

Practical models to calculate erosion threshold and erosion rate of non-cohesive sand-mud mixtures were developed based on models of pure sand/mud with addition of mud content effect (cohesive and packing effects). On the other hand, erosion threshold of cohesive sand-mud mixtures is linear interpolated between non-cohesive and pure-mud regimes while erosion rate is calculated based on pure-mud model. Besides, there are also another simpler formulations to calculate erosion threshold without distinction of non-cohesive and cohesive regimes (Ahmad et al., 2011; Wu et al., 2018). Regarding sand-silt mixtures, the critical bed-shear stress can be calculated using non-cohesive formula of Van Rijn (2007a) or applying an additional Van der Waals parameter into original Shields curve following Yao et al. (2022). The erosion rate of sand-silt mixtures primarily depends on permeability, void ratio and dry density of the mixed bed.

8. KNOWLEDGE GAPS

According to this literature review, the erosion and transport processes of mixed sediments have been proven to differ from those of pure sand or mud through numerous laboratory and field experiments. However, most studies have focused on sand-mud mixtures rather than sand-silt mixtures. In particular, the role of silt in the erosion of sand-silt mixtures remains unclear. The erosion thresholds and critical silt contents have been found to vary across multiple studies (Staudt, de Lange, Barzte). While experiments have frequently been conducted under current-only conditions with different sediment types, very few studies have examined wave-only or wave-current conditions. The role of waves and wave-induced currents in the erosion and transport of sand-mud or sand-silt mixtures has not been discussed in detail. Regarding practical models of sand-silt mixtures, Van der Waals forces have been considered in the erosion threshold, but the packing effects (or network structure) and RD have not yet been incorporated.

9. REFERENCES

Ahmad, M. F., et al. (2011), The Critical Shear Stresses for Sand and Mud Mixture.

Anthony, E. J., et al. (2015), Linking rapid erosion of the Mekong River delta to human activities. *Scientific Reports* **5**(1), 14745.

Barry, K. M., et al. (2006), Quasi-hydrodynamic lubrication effect of clay particles on sand grain erosion. *Estuarine, Coastal and Shelf Science* **67**(1), 161-169.

Bartzke, G., et al. (2013), On the Stabilizing Influence of Silt On Sand Beds. *Journal of Sedimentary Research* **83**(8), 691-703.

Colina Alonso, A., et al. (2024), A mud budget of the Wadden Sea and its implications for sediment management. *Communications Earth & Environment* **5**(1), 153.

Colina Alonso, A., et al. (2023), Morphodynamic Modeling of Tidal Basins: The Role of Sand-Mud Interaction. *Journal of Geophysical Research: Earth Surface* **128**(9), e2023JF007391.

de Lange, S. I., et al. (2024), Fine Sediment in Mixed Sand-Silt Environments Impacts Bedform Geometry by Altering Sediment Mobility. *Water Resources Research* **60**(7), e2024WR037065.

Flemming, B. W. (2000), A revised textural classification of gravel-free muddy sediments on the basis of ternary diagrams. *Continental Shelf Research* **20**(10), 1125-1137.

Jacobs, W., et al. (2011), Erosion threshold of sand–mud mixtures. *Continental Shelf Research* **31**(10, Supplement), S14-S25.

Kothyari, U. C. and R. K. Jain (2008), Influence of cohesion on the incipient motion condition of sediment mixtures. *Water Resources Research* **44**(4).

Le Hir, P., et al. (2005), Chapter 11 Erodibility of natural sediments: experiments on sand/mud mixtures from laboratory and field erosion tests. *Proceedings in Marine Science* **9**.

McCarron, C., et al. (2018), The hiding-exposure effect revisited: A method to calculate the mobility of bimodal sediment mixtures. *Marine Geology* **410**, 22-31.

Meyer-Peter, E. and R. Müller (1948), Formulas for bed-load transport, IAHSR 2nd meeting, Stockholm, appendix 2, IAHR.

Mitchener, H. and H. Torfs (1996), Erosion of mud/sand mixtures. *Coastal Engineering* **29**(1), 1-25.

Mohr, H., et al. (2018), The influence of permeability on the erosion rate of fine-grained marine sediments. *Coastal Engineering* **140**, 124-135.

Nguyen, V. L., et al. (2000), Late Holocene depositional environments and coastal evolution of the Mekong River Delta, Southern Vietnam. *Journal of Asian Earth Sciences* **18**(4), 427-439.

Panagiotopoulos, I., et al. (1997), The influence of clay on the threshold of movement of fine sandy beds. *Coastal Engineering* **32**(1), 19-43.

Parchure, T. M. and J. E. Davis (2005), Effect of organic materials on bulk density and erodibility of find sediment beds.

Parchure, T. M. and A. M. Teeter (2003), Lessons learned from existing projects on shoaling in harbors and navigation channels.

Partheniades, E. (1965), Erosion and Deposition of Cohesive Soils. *Journal of the Hydraulics Division* **91**(1), 105-139.

Perera, C., et al. (2020), Erosion rate of sand and mud mixtures. *International Journal of Sediment Research* **35**(6), 563-575.

Perkey, D., et al. (2020), *Erosion Thresholds and Rates for Sand-Mud Mixtures*.

Ribberink, J. S. (1998), Bed-load transport for steady flows and unsteady oscillatory flows. *Coastal Engineering* **34**(1), 59-82.

Roberts, J., et al. (1998), Effects of Particle Size and Bulk Density on Erosion of Quartz Particles. *Journal of Hydraulic Engineering* **124**(12), 1261-1267.

Shepard, F. P. (1954), Nomenclature based on sand-silt-clay ratios. *Journal of Sedimentary Research* **24**(3), 151-158.

Smith, J., et al. (2015), Erosion thresholds and rates for sand-mud mixtures. *Technical Report, U.S. Army Engineer Research and Development Center, Vicksburg, MS, USA*.

Soulsby, R. L. (1997), Dynamics of marine sands.

Staudt, F., et al. (2017), The role of grain-size ratio in the mobility of mixed granular beds. *Geomorphology* **278**, 314-328.

Staudt, F., et al. (2019), Effects of grain-size distribution and shape on sediment bed stability, near-bed flow and bed microstructure. *Earth Surface Processes and Landforms* **44**(5), 1100-1116.

Tamura, T., et al. (2010), Monsoon-influenced variations in morphology and sediment of a mesotidal beach on the Mekong River delta coast. *Geomorphology* **116**(1), 11-23.

te Slaa, S. (2020), Deposition and erosion of silt-rich sediment-water mixtures, Delft University of Technology.

Tian, Q., et al. (2021), Declining Sediment Discharge in the Yangtze River From 1956 to 2017: Spatial and Temporal Changes and Their Causes. *Water Resources Research* **57**(5), e2020WR028645.

Torfs, H. (1995), Erosion of mud/sand mixtures, Katholieke Universiteit Leuven, Leuven.

Torfs, H., et al. (1996), Settling and consolidation of mud/sand mixtures. *Coastal Engineering* **29**(1), 27-45.

Unverricht, D., et al. (2013), Modern sedimentation and morphology of the subaqueous Mekong Delta, Southern Vietnam. *Global and Planetary Change* **110**, 223-235.

Van Ledden, M. (2003), Sand-mud segregation in estuaries and tidal basins. *Communications on Hydraulic and Geotechnical Engineering* **3**.

Van Ledden, M., et al. (2004), A conceptual framework for the erosion behaviour of sand–mud mixtures. *Continental Shelf Research* **24**(1), 1-11.

Van Rijn, L. C. (1993), *Principles of sediment transport in rivers, estuaries and coastal seas*, Amsterdam, Aqua Publications.

Van Rijn, L. C. (2007a), Unified View of Sediment Transport by Currents and Waves. I: Initiation of Motion, Bed Roughness, and Bed-Load Transport. *Journal of Hydraulic Engineering* **133**(6), 649-667.

Van Rijn, L. C. (2020), Erodibility of Mud–Sand Bed Mixtures. *Journal of Hydraulic Engineering* **146**(1), 04019050.

Van Rijn, L. C. C. A., A.

van Maren, D. (2020), Literature Review MUSA: on the Interaction between Mud and Sand. *MUSA Project.*

Wentworth, C. K. (1922), A Scale of Grade and Class Terms for Clastic Sediments. *The Journal of Geology* **30**(5), 377-392.

Williamson, H. J. and M. C. Ockenden (1993), Laboratory and field investigations of mud and sand mixtures. *Advances in Hydro-science and Engineering* **1**, 622-629.

Winterwerp, J. C., et al. (2021), *Fine Sediment in Open Water*, WORLD SCIENTIFIC.

Wu, W., et al. (2018), Critical shear stress for erosion of sand and mud mixtures. *Journal of Hydraulic Research* **56**(1), 96-110.

Yao, P., et al. (2018), Erosion Behavior of Sand-silt Mixtures: the Role of Silt Content. *Journal of Coastal Research*(85 (10085)), 1171-1175.

Yao, P., et al. (2022), Erosion Behavior of Sand-Silt Mixtures: Revisiting the Erosion Threshold. *Water Resources Research* **58**(9), e2021WR031788.

Yao, P., et al. (2015), Experiment inspired numerical modeling of sediment concentration over sand–silt mixtures. *Coastal Engineering* **105**, 75-89.

Ye, L., et al. (2023), Biophysical flocculation reduces variability of cohesive sediment settling velocity. *Communications Earth & Environment* **4**(1), 138.

Zuo, L., et al. (2017), On incipient motion of silt-sand under combined action of waves and currents. *Applied Ocean Research* **69**, 116-125.